

Conformational analysis and docking study of potent factor XIIIa inhibitors having a cyclopropenone ring

Yoriko Iwata,* Keiko Tago,* Toshihiro Kiho,* Hiroshi Kogen,* Tomoyuki Fujioka,† Noriko Otsuka,† Keiko Suzuki-Konagai,* Takeshi Ogita,* and Shuichi Miyamoto*

*Exploratory Chemistry Research Laboratories, Sankyo Co., Ltd., 1-2-58, Hiromachi, Shinagawa-ku, Tokyo 140-8710, Japan

†Pharmacological and Molecular Biological Research Laboratories, Sankyo Co., Ltd., 1-2-58, Hiromachi, Shinagawa-ku, Tokyo 140-8710, Japan

A conformational analysis and docking study of potent factor XIIIa inhibitors having a cyclopropenone ring were carried out in an attempt to obtain structural insight into the inhibition mechanism. First, stable conformers of the inhibitors alone were obtained from the conformational analysis by systematic search and molecular dynamics. Next, a binding form model of factor XIIIa was built based on an X-ray crystal structure of the enzyme. Finally, the docking study of the inhibitors into the model's binding site was performed. From the resulting stable complex structures, it was found that the cyclopropenone ring fits the active site located at the base of the binding cavity with high complementarity. The carbonyl oxygen of the cyclopropenone ring formed a hydrogen bond to the indole NH group of Trp279 and the terminal carbon atom of the reactive C=C double bond was in close proximity to the sulfur atom of the catalytic residue, Cys314. This binding mode suggests a possible inhibition mechanism, whereby the cysteine residue reacts with the cyclopropenone ring of the inhibitor, forming an enzyme-ligand adduct. In addition, the higher interaction energies between factor XIIIa and the inhibitors alluded to the probable binding sites of the ligand side chain. © 2000 by Elsevier Science Inc.

Keywords: conformational analysis, docking study, molecular mechanics, systematic search, molecular dynamics, factor XIIIa inhibitor, cyclopropenone

Color Plates for this article are on pages 602–604.

Corresponding author: Shuichi Miyamoto, Exploratory Chemistry Research Laboratories, Sankyo Co., Ltd., 1-2-58, Hiromachi, Shinagawa-ku, Tokyo 140-8710, Japan. Tel.: +81-3-3492-3131; fax: +81-3-5436-8570.

E-mail address: miya@shina.sankyo.co.jp (S. Miyamoto)

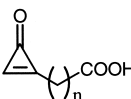
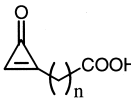
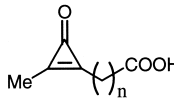
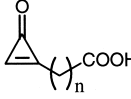
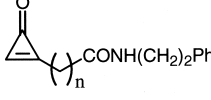
INTRODUCTION

Factor XIII is a transglutaminase that acts on the final step in the blood coagulation cascade.^{1–3} In contrast to all other enzymes involved, it is not a serine protease but a thiol enzyme and activated to factor XIIIa by thrombin in the presence of Ca²⁺.^{4,5} Factor XIIIa covalently cross-links fibrin monomers and converts soft fibrin clots to hard clots.^{6–8} These clots are less rapidly lysed by agents like plasmin or tissue plasminogen activator. In addition, factor XIIIa is also known to cross-link fibrin to extracellular matrixes, such as vitronectin, fibronectin, and collagen, thereby forming additional clots to the vessel wall. Specific inhibitors of factor XIIIa are therefore thought to offer possibilities in the therapy for thrombosis,¹ atherosclerosis, and coronary heart disease^{9,10} and a few such inhibitors have already been reported. Although several peptides are known to inhibit factor XIIIa,^{11,12} examples of specific non-peptide inhibitors are few.¹³

In the search for specific inhibitors of factor XIIIa, we have isolated alutacenoic acids A (**1**) and B (**2**) (Table 1), a pair of fungal metabolites from *Eupenicillium alutaceum* Scott SANK 23495.¹⁵ They were found to be potent specific inhibitors of factor XIIIa and, surprisingly, they were mono-substituted cyclopropenone derivatives with aliphatic tethers attached to a terminal carboxylic acid. We synthesized **1**, **2**, and their derivatives and studied the structure–activity relationships by varying the chain length between the ring and the carboxyl group.¹⁵ Among the compounds obtained, **5** was found to be one of the most potent nonpeptide inhibitors ever discovered.

The detailed mechanism of the enzyme inhibition by compounds with a cyclopropenone skeleton is still unknown. Since the inhibitory activity was lost by the replacement of the cyclopropenone ring with an epoxy ring (unpublished data), the cyclopropenone ring was considered to be necessary for the inhibition. Introduction of a methyl group into the reactive

Table 1. Factor XIIIa inhibitory activities of cyclopropanone derivatives

Compound	Structure	n	IC ₅₀ ^a (μM)
1		5	1.9
2		7	0.61
3		7	>10000
4		10	0.31
5		7	0.026

^a IC₅₀ was determined according to reference 14.

C=C double bond also brought about the inactivation of the compound as exemplified with compound **3**. A full kinetic analysis of **5** revealed that this was a time-dependent (i.e., irreversible) inhibitor of factor XIIIa with a second-order inhibition rate constant (k_{inact}/K_i) of 5080 s⁻¹·M⁻¹.¹⁵ It should be noted that factor XIIIa has a cysteine residue in its catalytic center. Considering the above, it was presumed that the inhibition was caused by the reaction of the enzyme's cysteine residue with the ligand's cyclopropanone ring. We therefore carried out a docking study to examine whether the inhibitors could adopt a docking mode in which such a reaction could proceed and, furthermore, determine where the alkyl side chain might be located to pursue the inhibitor design.

Factor XIII exists as a homodimer of two A subunits in platelets and monocytes. The plasma enzyme is a tetramer of two A and two B chains. Upon the activation of both forms of factor XIII via proteolysis, a 37-residue amino-terminal peptide, i.e., an activation peptide, is released.^{4,5} In the case of the plasma form, dissociation of the B chains occurs as well. The enzyme catalyzes the formation of isopeptide bonds between the side chains of glutamine and lysine residues in a variety of proteins.

X-ray crystallographic analyses of factor XIII zymogen were done by two research groups and six 3D structures of factor XIII were registered in the Protein Data Bank¹⁶ as of June 1999. All of them were inactive cellular forms consisting of two A subunits with the activation peptide over the active site. Some of them had different metal ions (Ca²⁺, Sr²⁺, and Yb³⁺) located in an ion-binding site, but no organic ligand was observed in all cases. The A subunit of 730 amino acids is made up of four distinct and sequential domains: β-sandwich, core, barrel-1, and barrel-2. The identified catalytic center comprising residues Cys314, His373, and Asp396 are completely buried and inaccessible to the substrate.^{17–19}

Even after the hypothetical removal of the activation peptide, the active site is still inaccessible because the side chain of Tyr560 in the barrel-1 domain is in close proximity to Cys314 in the catalytic center. Yee et al.¹⁷ suggested that upon activation, the peptide linking the core and barrel-1 domain undergoes a conformational change and it causes the barrel-1 domain to rotate away from the core, making the active site accessible to ligands. It was also observed that thrombin or a trypsin-cleaved factor XIII fragment (corresponding to the core and sandwich domains) possessed catalytic activity.²⁰ We therefore decided to build a model enzyme to which ligands could bind, so that a docking study could be performed.

In this article, we report the detailed results of the conformational analysis and the docking study of a series of inhibitors, although the synthesis and the biological activities of the inhibitors and a complex structure model will be communicated briefly elsewhere.¹⁵ Chemical structures and factor XIIIa inhibitory activities of five analyzed compounds (**1–5**) are shown in Table 1. The conformational analysis was carried out with systematic search and molecular dynamics simulations. In principle, the docking study of the inhibitors was carried out manually. For the least flexible compound **1**, the docking mode analysis by systematic search was also performed and compared with the manual docking. By using the global minimum energies of the inhibitors, the interaction energies between factor XIIIa and the inhibitors were estimated and compared with the inhibitory activities.

METHODS

Molecular mechanics and molecular dynamics calculations with an all-atom force field were performed using the QUANTA/CHARMM system²¹ with the supplied parameter set, except for the changes noted. A distance dependent dielectric constant of 4r was used. The Adopted-Basis Newton Raphson algorithm²² was employed for minimization in molecular mechanics calculations with an energy gradient tolerance of 0.01 kcal · mol⁻¹ · Å⁻¹. A nonbonded cutoff of 15 Å with the switching function on at 11 Å and off at 14 Å was used. Quantum mechanics calculations were carried out with the Spartan program.²³

Conformational Analysis of Inhibitors

Because the cyclopropanone structure is rather unique, some of the bond angle parameters for the CHARMM force field were missing or inappropriate. Additional or modified force field parameters were derived from the analogous structures^{24–26} of the Cambridge Crystal Structure Database²⁷ and are given in Table 2. The carboxylic acid of the inhibitors was model-built in an anion form. Chemical structures and torsional angle definitions of cyclopropanone derivatives used in this study are shown in Figure 1. The partial atomic charges of compounds **1–5** were assigned with the charge templates in QUANTA and are shown in Figure 2a.

With respect to **1**, **2**, and **3**, an exhaustive conformational analysis was carried out by systematic search. The torsional angles of the initial structures were changed as shown in Figure 1 with the grid scan option in QUANTA. As for **4** and **5**, a conformational analysis with molecular dynamics was performed. The system was heated to 600 K for 2.4 ps followed by an equilibration during 10 ps. A production run of 1200 ps was

Table 2. Additional angle force field parameters used for cyclopropenone structure

	Angle		K (kcal mol ⁻¹ rad ⁻²)	θ (deg)
OK	C3	CUA1	55	152.5
CUA1	C3	CUA1	55	55.0
C3	CUA1	CUA1	55	62.5
CT	CUA1	CUA1	40	150.2
CT	CUA1	C3	40	147.3
C3	CUA1	HA	35	147.3
CUA1	CUA1	HA	35	150.2

then carried out. A time step of 1 fs was used and the coordinates were saved at every 0.2 ps. The simulations were repeated with two different kinds of starting conformations. In the systematic search and molecular dynamics approach, all the generated and saved initial structures were geometry-optimized by molecular mechanics. Cluster analysis of the resulting stable conformers of the inhibitors was done based on the torsional angles as shown in Figure 1 with a threshold of 30° to give unique stable conformers.

Modeling of the binding form of factor XIII

The crystal structures of factor XIII in the Protein Data Bank were almost identical. For the modeling of the binding form, 1F13¹⁹ was used due to its having the highest resolution (2.1 Å). In addition to the N-terminal activation peptide, the entire barrel-1 domain was removed from the crystal structure. The dimer model structure thus built had more than one thousand residues. To simplify manipulation in the docking study, a model with residues within 20 Å from the sulfur atom of Cys314 was constructed. Hydrogen atoms were added to the model in progress and geometry-optimized to afford the final binding form model of factor XIIIa. The model was named RmvB1. The stereo plot of the active site region is given in Color Plate 1.

It was suggested that Cys314 in the catalytic site was negatively charged, i.e., was in the thiolate form from the X-ray crystallographic analysis, by Yee et al.,¹⁷ who reported a thorough examination of the active site. We therefore determined the partial atomic charges of the thiolate cysteine residue. Geometry optimization with the semiempirical molecular orbital method PM3 was performed on the thiolate form of Cys314.²³ A single-point *ab initio* calculation was then carried out with a 6-31G** basis set using the Hartree-Fock theory to obtain the electrostatic potential charges. By adjusting them to be fitted to the standard amino acid residue in the CHARMM force field, the partial atomic charges were determined as shown in Figure 2b.

Docking Study of the Inhibitors into the Binding Form Model of Factor XIIIa

The docking study of the inhibitors was manually carried out with the QUANTA/CHARMM system. Initial positions and conformations of the inhibitors were manually set and stable complex structures were obtained by energy minimization with

the enzyme model atoms being fixed. Several low energy conformations of the inhibitors, including the global minimum energy conformation, were evaluated in this manner.

As for **1**, a docking mode analysis by systematic search within the active site was performed as well. Taking one of the stable complex models constructed by the manual docking as a starting structure, the torsional angles of **1** were changed with the grid scan option in the same way as in the analysis of the isolated inhibitor. The resulting initial structures were then energy-minimized with the fixed enzyme model to afford a series of stable complex structures. Cluster analysis of the ligand docking modes was done based on the RMS deviations of three atoms, O1, C2, and C9, of **1** with a threshold of 1.5 Å.

The interaction energy between factor XIIIa and the inhibitor was estimated by simply subtracting the conformational energies of the enzyme and the isolated inhibitor from that of the complex. The global minimum energy obtained by the conformational analysis was used as the conformational energy of the isolated inhibitor. In the actual derivation of the interaction energy, the conformational energy of the enzyme was not subtracted because it was common to all.

HOMO/LUMO Calculations of the Cysteine Residue and the Cyclopropenone Model

As for the cysteine residue in the thiolate form, the above geometry-optimized structure with the semiempirical molecular orbital method PM3 was used. A single-point *ab initio* calculation was carried out with a 6-31G** basis set using the Hartree-Fock theory to obtain the HOMO.²³ With respect to the cyclopropenone structure, the model compound **6** (Figure 1) with $\tau_1 = +gauche$ was used. Geometry optimization by the *ab initio* method with a 6-31G* basis set was performed using the Hartree-Fock theory.²³ The LUMO was then calculated with the same basis set.

RESULTS AND DISCUSSION

Conformational Analysis of Inhibitors

The exhaustive conformational analysis by systematic search was carried out for **1**, **2**, and **3**. For **4** and **5**, however, it was rather hard to apply the same approach. These compounds had such long alkyl chains that a huge number of initial conformations had to be handled. Conformational analysis with molecular dynamics was therefore performed on them. As many as 251, 1872, 1877, 3491, and 4747 unique stable conformations were obtained for **1**, **2**, **3**, **4**, and **5**, respectively. The resulting global minimum energy structure of each inhibitor was used to estimate the interaction energy in the docking study. The most stable conformer for each molecule is shown in Figure 3.

As seen in Figure 3, simple methylene chains of the inhibitors were liable to take *trans* conformations as expected. Interestingly, the conformations with the lowest energy had $\tau_1 = gauche$ ($\pm 60^\circ$) except for **3** with $\tau_1 = trans$ (180°). It should be noted that τ_1 was defined as C1-C3-C4-C5 (see compound **1** in Figure 1). If we took it as C2-C3-C4-C5, the *gauche* ($\pm 120^\circ$) conformation would be slightly lower (0.2 kcal/mol) in energy than the *cis* (0°) conformation, except for **3**. Although all global minimum conformers had $\tau_2 = \pm gauche$, energy differences between *trans* and *gauche* conformers were very small (around 0.1 kcal/mol).

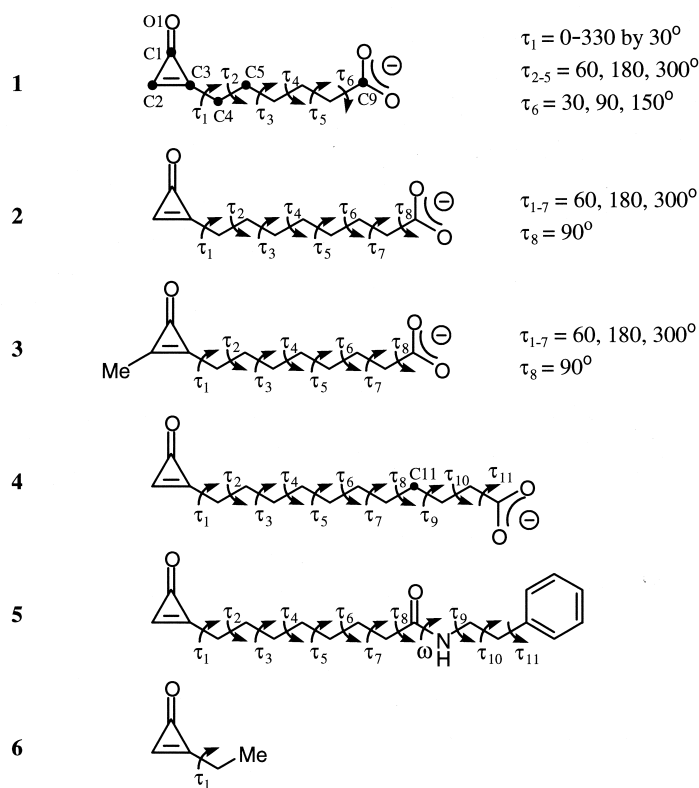


Figure 1. Chemical structures and torsional angle definitions of cyclopropenone derivatives, together with values assigned in the systematic search.

Docking Study of the Inhibitors into the Binding Form Model of Factor XIIIa

The docking study of the inhibitors into the binding form model, RmvB1, was carried out manually. Since we assumed that the inhibition was caused by the reaction of the cysteine residue with the cyclopropenone ring, we concentrated on the binding modes in which the cyclopropenone ring was located in the vicinity of Cys314. Among the atoms of the catalytic triad, only the side chain atoms of Cys314 were accessible to ligands even after the removal of the barrel-1 domain. Cys314 sits in the small basin at the base of the presumed binding cavity. The orientation of the cyclopropenone ring in the basin was, therefore, so restricted that the selection of the most favorable binding mode was rather straightforward.

On the other hand, there was little positional restriction with respect to the ligand side chain. After a series of manual investigations, it was found that there were four main binding sites (A, B, C, and D), where stable complexes could be formed. The locations of these sites are shown schematically in Figure 4. Even in the intact enzyme structure with the barrel-1 domain, all four sites were so close to the enzyme surface that they are presumed to be easily accessible to the ligands by a small movement of the barrel-1 domain. In sites B and C, the alkyl chain of the ligand extended to the position where the activation peptide was originally situated.

It is possible that the sites derived from the manual docking study may be biased. For **1** with fewer degrees of freedom, a docking study by systematic search was performed and compared with the manual docking to achieve an unbiased docking.

The resulting docking modes were classified into eight clusters. Five of these clusters corresponded to the four sites derived above; two of the clusters had side chains pointed to the removed barrel-1 domain; and the alkyl chains in the last cluster had no direct interactions with the enzyme surface residues in the binding pocket. In addition, the last three modes were not energetically favored ($\Delta E = 7-13 \text{ kcal/mol}$). Therefore, they were not considered for the manual docking.

With respect to the five clusters corresponding to sites A-D, conformational energies of the complexes were compared with those afforded by the manual docking. In both docking approaches, the most stable complexes were those bound to site D. They were also found to have the same energy. In the other sites as well, stable complexes with comparable energies ($\sim \pm 2 \text{ kcal/mol}$) were obtained by both methods. Considering the above, we concluded that the four binding sites and conformational energies derived by the manual docking were reasonable.

For **2** and **5**, conformational energies of several complex structures were calculated by using the initial whole dimer structure without the barrel-1 domain. As a result, nearly identical ligand conformations and complex energies were obtained compared with those using the RmvB1 model. This indicates that the RmvB1 model with a radius of 20 Å was sufficient for the current purpose. As for **2**, an alternative binding mode with the flipped cyclopropenone ring was examined. The conformational energy of that binding mode was, however, 3 kcal/mol higher than that obtained before and therefore the flipped binding mode was not considered any further.

a

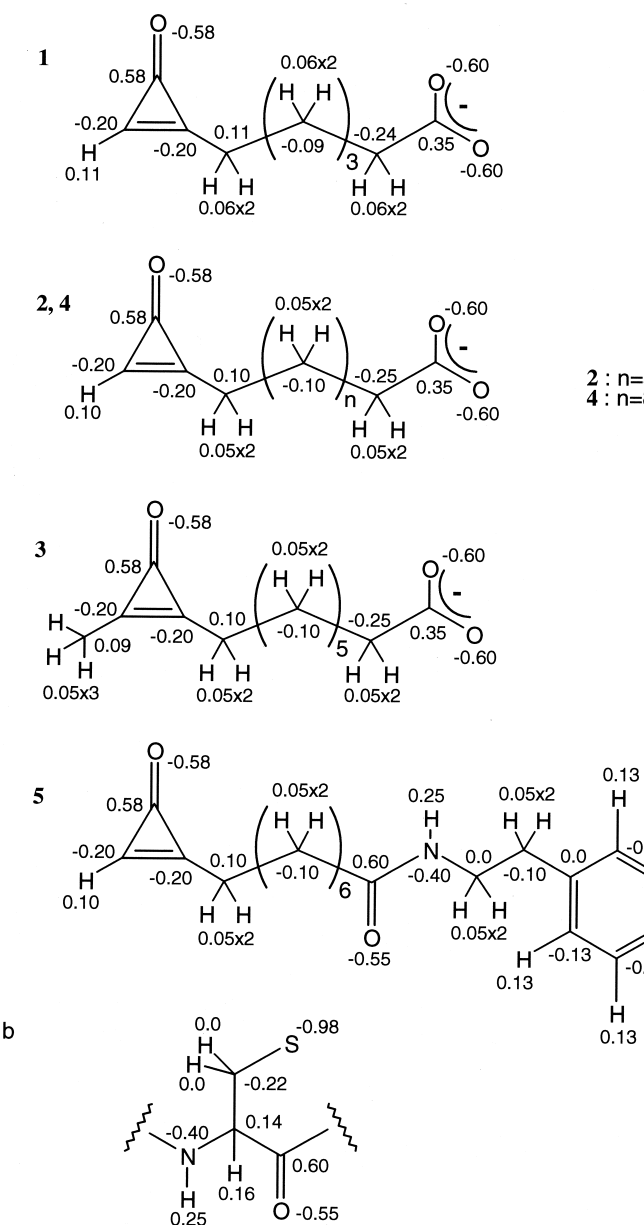


Figure 2. Partial atomic charges used in this study.
(a) cyclopropenone derivatives. (b) cysteine residue in the thiolate form.

We employed manual docking and docking by systematic search since we assumed that the cyclopropenone moiety was in the vicinity of the catalytic Cys314, which sits in the small basin located at the base of the presumed binding cavity. Another docking program, UCSF DOCK,²⁸ is not designed to search docking modes where a certain moiety of the docked molecule is restricted to a certain part of the target protein. Furthermore, our docking by systematic search corresponds to flexible systematic docking, where the cyclopropenone head is fixed with the side chain tail in several different positions. These are the reasons that we adopted the current approaches.

Complex Structure and Inhibition Mechanism

The complex structure models of RmvB1 and the more potent inhibitors **4** and **5** as well as the inactive **3** are presented in

Color Plates 2–5. Color Plate 2 shows the most stable complex structure model of **5** obtained by manual docking in site A. It can be seen from the color plate that the cyclopropenone ring is located in the active site at the base of the binding pocket and the alkyl side chain stretches along the groove. The terminal phenyl ring is positioned in the hydrophobic region, which consists of Met350, Ile352, Val369, and Leu439. Color Plate 3 is an enlarged view of the catalytic center and shows that the cyclopropenone moiety fits with high complementarity into the small basin. The carbonyl oxygen (O1) of the cyclopropenone ring forms a hydrogen bond with the indole NH of Trp279 (the O1–Nε1 distance is 2.9 Å). This oxygen atom position is close to the position in which the hydroxy oxygen of Tyr560 of the barrel-1 domain was originally located. This hydroxy oxygen is also hydrogen-bonded to the indole NH of Trp279 in the intact dimer structure. The reactive terminal carbon atom (C2) is in

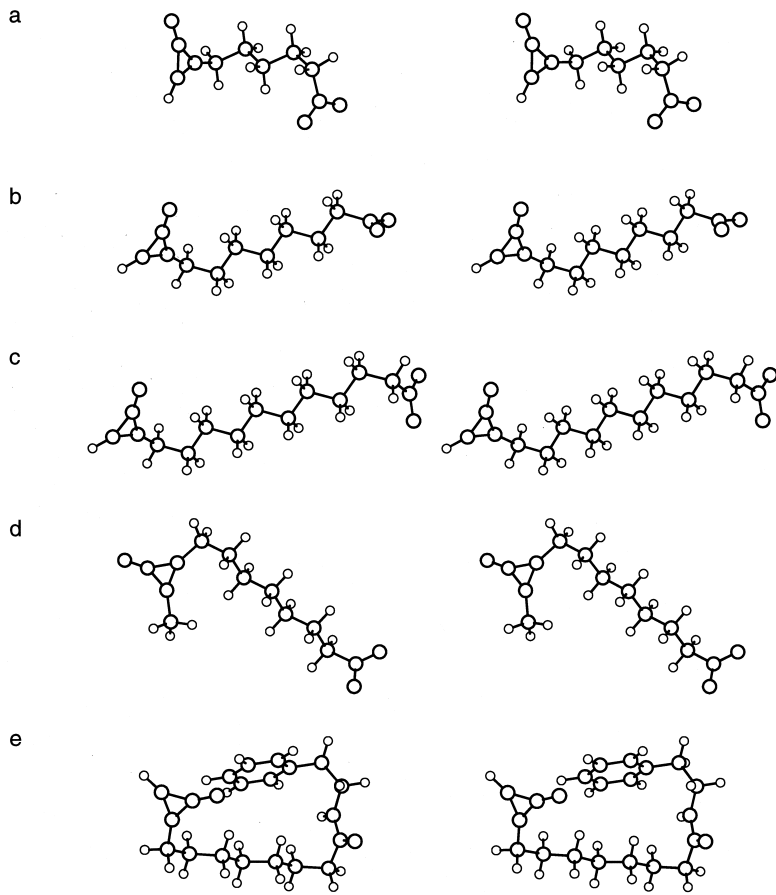


*Figure 3. Stereofigures of the most stable conformations of **1–5**.*

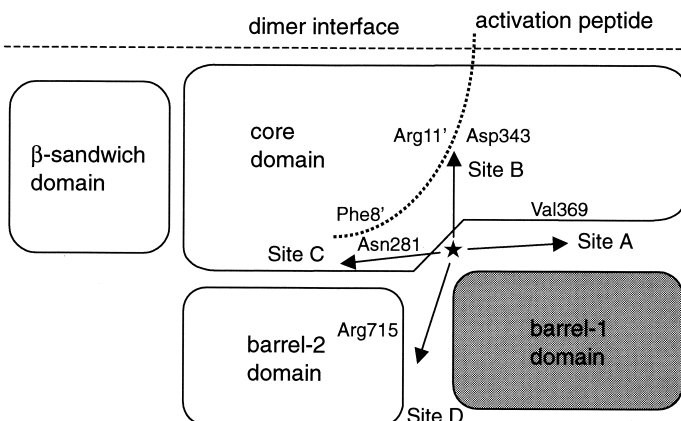
close proximity to the sulfur atom ($S\gamma$) of Cys314 where the $C2-S\gamma$ distance is 2.9 Å. This is much shorter than the sum (3.9 Å) of Van der Waals radii of $C2$ and $S\gamma$.

The lowest energy complex structure of **4** in site B is illustrated in Color Plate 4, which shows that the cyclopropane ring fits well into the active site. A hydrogen bond is formed between the O1 of the inhibitor and the indole NH of Trp279 (the O1–N ϵ 1 distance is 3.0 Å). The reactive carbon atom (C2) is close vicinity to the $S\gamma$ of Cys314 (the $C2-S\gamma$ distance is 3.1 Å). The alkyl chain of **4** had hydrophobic interactions with the aromatic rings of Trp279 and Trp370. The interaction energy of **5** when it adopts a binding mode equiv-

alent to **4** shown in Color Plate 4 was 2 kcal/mol lower than that of **4**. In the case of site A, the interaction energy of **4** when it adopts a binding mode similar to **5** shown in Color Plate 2 was 4 kcal/mol higher than that of **5**.

Color Plate 5 shows the active site of the complex structure of the inactive compound **3** with the aliphatic side chain in site B. As seen in Color Plate 5, the cyclopropanone ring with a methyl substituent does not fit well into the catalytic cavity, leaving a gap between the enzyme and the ligand. The hydrogen bond between the carbonyl oxygen and the NH of Trp279 is broken and the $C2-S\gamma$ distance is extended to 4.5 Å, due to the extra methyl group located at the very bottom of the cavity.

Figure 4. Schematic representation of the ligand binding sites of factor XIIIa. ★ represents Cys314 in the active site.



The above structural feature suggests a possible enzyme inhibition mechanism as shown in Figure 5, where the inhibition is caused by a Michael addition of the thiolate of Cys314 onto the C=C double bond of the inhibitor, forming an enzyme-ligand adduct. The NH group of Trp279 is considered to play an important role in positioning the cyclopropenone ring properly and facilitating the reaction by drawing the electrons of the carbonyl oxygen. In the case of the inactive compound **3**, the extra methyl group at the terminal site is assumed to prevent the carbonyl oxygen from hydrogen-bonding to the NH group and the double bond from approaching the sulfur atom. Trp279 is conserved among the transglutaminase family^{3,29} and it was postulated as a component of the “oxyanion hole” that stabilizes reaction intermediates, by comparison with the papain crystal structures.³⁰ The side chain amide group of a glutamine residue, which is one of the substrates of factor XIIIa, may bind in the same fashion as shown in Color Plate 3.

To begin to elucidate the definite inhibition mechanism of the cyclopropenone compounds, we have carried out preliminary molecular orbital calculations on the cyclopropenone and the cysteine residue in the thiolate form. The results indicated that the LUMO of the former and the HOMO of the latter were located on the C=C double bond and Sγ, respectively. This is consistent with the proposed mechanism described above, and illustrated in Figure 5. Another possible reaction mechanism is the addition of the thiolate onto the carbonyl bond of the inhibitor, forming a different enzyme-ligand adduct. Since the distance from the Sγ to the carbonyl carbon atom (C1) is 0.4 Å longer than the distance to the C2 in the C=C double bond (Color Plate 3) and the LUMO is located, not on the carbonyl group, but on the C=C double bond, we considered that this inhibition mechanism is less plausible. The enzyme inhibition mechanism may be verified if the characterization of the factor XIIIa inactivated by the radiochemically labeled cyclopropenone analogs are carried out. Freund et al.¹³ had found 2-[(2-oxopropyl)thio]-imidazolium derivatives to possess inhibitory activities against factor XIIIa with a potency similar to **5**. Although it was reported that these compounds exhibited their inhibitory activities by reacting with the catalytic thiol group to form enzyme-ligand adducts, their reaction mechanism was considered to be different from our compounds. Besides the inhibition mechanism, it is also useful for the design of factor XIIIa inhibitors that the possible docking modes are visually presented in this study.

Interaction Energy and Side Chain Binding Site

In Table 3, the maximum interaction energy obtained in each biding site (sites A-D) is listed for the respective compound together with the inhibitory potency (IC_{50}). If we assume the inhibition mechanism proposed above, the IC_{50} values should correlate not to the interaction energies but to the reaction energies of the ligands with the enzyme. However, it was rather hard to estimate the reaction energies. Since the reaction moieties of the ligands are identical except for **3**, the reaction energies are considered to be comparable. In this case, the reaction rate can be adequately approximated by the interaction energy immediately prior to the reaction. Furthermore, Freund et al.¹³ had indicated that 2-[(2-oxopropyl)thio]imidazolium derivatives might form a complex with factor XIIIa before the irreversible inactivation based on the kinetic analysis of the inhibition. Therefore, the correlation between the IC_{50} and the maximum interaction energies were considered.

As seen in Table 3, as the interaction energy increases, the inhibitory potency in site A and site B tends to rise as well. In site C, interaction energies were small compared with those in the other sites and the above tendency was not observed. In site D, the terminal carboxylic acid of ligands had a favorable ionic interaction with the guanidium group of Arg715. This seemed to be the reason that a relatively small interaction energy was obtained for the most potent inhibitor **5**, which has no terminal carboxylic acid. In fact, in the intact crystal structure including the barrel-1 domain, Arg715 had an ionic interaction with Glu60.

Interestingly, with regard to the two factor XIIIa substrates, both the glutamine and lysine substrates have long alkyl chains as in our inhibitors, which suggest that sites A and B or even C and D might correspond to the substrate binding sites. Muszbek et al.²⁹ reported that the position of Arg11' and the chemical similarity between the side chain groups of arginine and lysine residues suggested the direction from which the lysine-containing substrate approached. This direction points to site B as illustrated in Figure 4. In fact, the carbon atom (C11) of **4** shown in Color Plate 4 was within 0.7 Å from the position in which the Cα of Arg11' of the activation peptide was originally situated. Yee et al.¹⁷ postulated that the catalytic Cys314 could be approached by the glutamine substrate macromolecule from the direction of the β-barrel domains. Site A might correspond to this direction. However, site D might be an alternative binding site for the glutamine substrate because it is

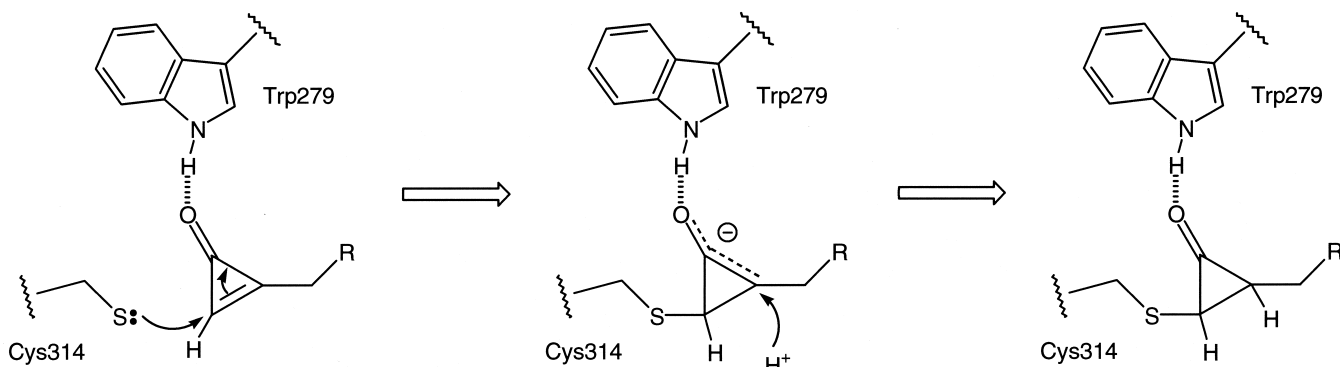


Figure 5. Possible reaction pathway between the catalytic site of Factor XIIIa and the inhibitor cyclopropenone ring.

Table 3. Interaction energies between the binding form model of factor XIIIa and its inhibitors

Compound	IC_{50} (μM)	ΔE (kcal/mol)			
		Site A	Site B	Site C	Site D
3	>10000	-16.8	-17.7	-13.2	-25.3
1	1.9	-21.3	-19.1	-24.1	-26.8
2	0.61	-22.3	-20.2	-18.6	-30.2
4	0.31	-24.9	-23.4	-21.7	-30.8
5	0.026	-28.7	-31.6	-25.7	-27.1

located opposite to site B if the lysine-containing substrate binds to site B first.

Although further experimental studies would be necessary to determine the definite binding site of the side chains of our compounds, the complex structures presented in this study may be useful for the design of such experiments and new inhibitors as well. In addition to the static analysis of the binding sites discussed above, it would be interesting to examine how the barrel-1 domain rotates or deforms with respect to the core domain, by performing molecular dynamics simulations of the entire factor XIIIa structure. Such a dynamic structure of the enzyme might elucidate the more accessible parts to the ligands.

ACKNOWLEDGMENTS

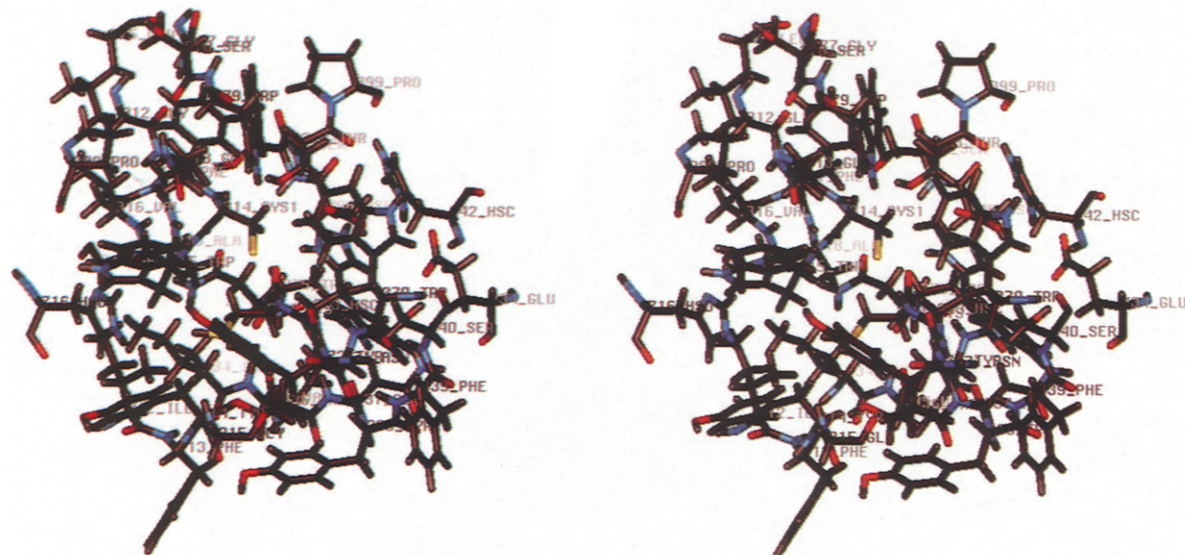
We thank Dr. Atsushi Kasuya for helpful discussions.

REFERENCES

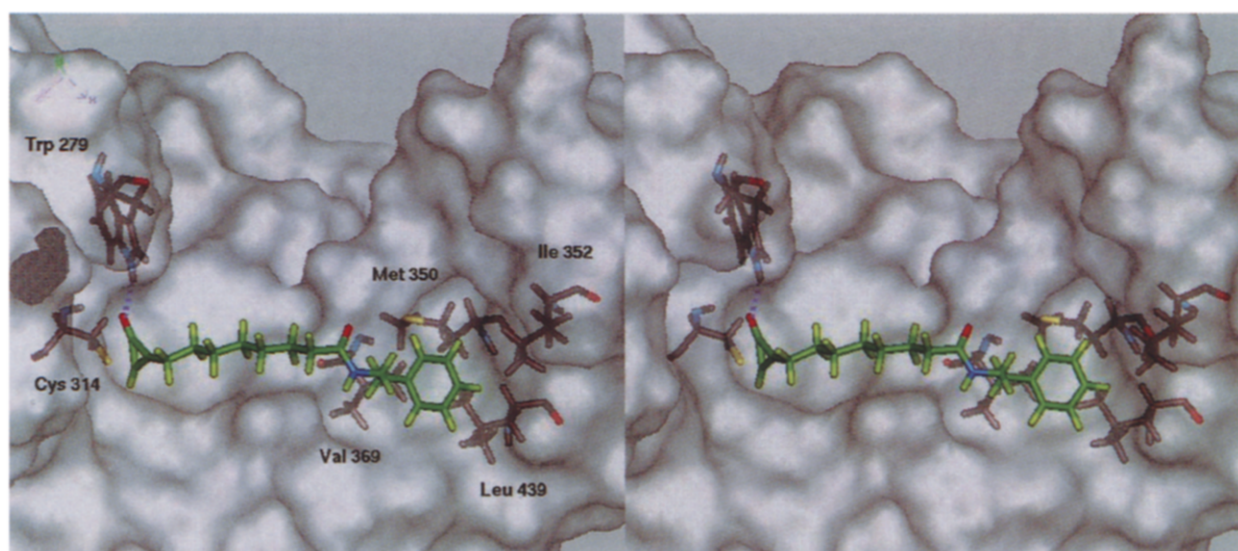
- Leidy, E.M., Stern, A.M., Friedman, P.A., and Bush, L.R. Enhanced thrombolysis by a factor XIIIa inhibitor in a rabbit model of femoral artery thrombosis. *Thromb. Res.* 1990, **59**, 15–26
- Greenberg, C.S., Birckbichler, P.J., and Rice, R.H. Transglutaminases: multi-functional cross-linking enzymes that stabilize tissues. *FASEB J.* 1991, **5**, 3071–3077
- Aeschliman, D., and Paulsson, M. Transglutaminases: Protein cross-linking enzymes in tissues and body fluids. *Thromb. Haemostasis* 1994, **71**, 402–415
- Takagi, T., and Doolittle, R.F. Amino acid sequence on factor XIII and the peptide released during its activation by thrombin. *Biochemistry* 1974, **13**, 750–756
- Credo, R.B., Curtis, C.G., and Lorand, L. Ca^{2+} -related regulatory function of fibrinogen. *Proc. Natl. Acad. Sci. USA* 1978, **75**, 4234–4237
- Bruner-Lorand, J., Pilkington, T.R.E., and Lorand, L. Inhibitors of fibrin cross-linking: Relevance for thrombolysis. *Nature (London)* 1966, **210**, 1273–1274
- Gladner, J.A., and Nossel, R. Effects of crosslinking on the rigidity and proteolytic susceptibility of human fibrin clots. *Thromb. Res.* 1983, **30**, 273–288
- Shen, L., and Lorand, L. Contribution of fibrin stabilization to clot strength. *J. Clin. Invest.* 1983, **71**, 1336–1341
- Francis, C.W., Connaghan, D.G., Scott, W.L., and Marder, V.J. Increased plasma concentration of cross-linked fibrin polymers in acute myocardial infarction. *Circulation* 1987, **75**, 1170–1177
- Kloczko, J., Wojtukiewicz, M., Bielawiec, M., and Zuch, A. Alterations of haemostasis parameters with special reference to fibrin stabilization, factor XIII and fibronectin in patients with obliterative atherosclerosis. *Thromb. Res.* 1988, **51**, 575–581
- Achyuthan, K.E., Slaughter, T.F., Santiago, M.A., Englund, J.J., and Greenberg, C.S. Factor XIIIa-derived peptides inhibit transglutaminase activity. *J. Biol. Chem.* 1993, **268**, 21284–21292
- Finney, S., Seale, L., Sawyer, R.T., and Wallis, R.B. Tridegin, a new peptidic inhibitor of factor XIIIa, from the blood-sucking leech *Haementeria ghilianii*. *Biochem. J.* 1997, **324**, 797–805
- Freund, K.F., Doshi, K.P., Gaul, S.L., Claremon, D.A., Remy, D.C., Baldwin, J.J., Pitzenberger, S.M., and Stern, A.M. Transglutaminase inhibition by 2-[$(2$ -oxopropyl)thio]-imidazolium derivatives: Mechanism of factor XIIIa inactivation. *Biochemistry*, 1994, **33**, 10109–10119
- Usui, T., Takagi, J., and Saito, Y. Propolyptide of von Willebrand factor serves as a substrate for factor XIIIa and is cross-linked to laminin. *J. Biol. Chem.* 1993, **268**, 12311–12316
- Kogen, H., Kiho, T., Keiko Tago, K., Miyamoto, S., Fujioka, T., Otsuka, N., Keiko Suzuki-Konagai, K., and Ogita, T. Alutacenoic acids A and B, rare naturally occurring cyclopropenone derivatives isolated from fungi: Potent non-peptide factor XIIIa inhibitors. *J. Am. Chem. Soc.* 2000, **122**, 1842–1843
- Bernstein, F.C., Koetzle, T.F., Williams, G.J.B., Meyer, E.F. Jr., Brice, M.D., Rodgers, J.R., Kennard, O., Shimanouchi, T., and Tasumi, M. The protein data bank: A computer-based archival file for macromolecular structures. *J. Mol. Biol.* 1977, **112**, 535
- Yee, V.C., Pedersen, L.C., Le Trong, I., Bishop, P.D., Stenkamp, R.E., and Teller, D.C. Three dimensional structure of a transglutaminase: Human blood coagulation factor XIII. *Proc. Natl. Acad. Sci. USA* 1994, **91**, 7296–7300
- Yee, V.C., Pedersen, L.C., Bishop, P.D., Stenkamp, R.E., and Teller, D.C. Structural evidence that the activation peptide is not released upon thrombin cleavage of factor XIII. *Thromb. Res.* 1995, **78**, 389–397
- Weiss, M.S., Metzner, H.J., and Hilgenfeld, R. Two non-proline *cis* peptide bonds may be important for factor XIII function. *FEBS Lett.* 1998, **423**, 291–296
- Greenberg, C.S., Enghild, J.J., Mary, A., Dobson, J.V., and Achyuthan, K.E. Isolation of a fibrin-binding fragment from blood coagulation factor XIII capable of cross-linking fibrin(ogen). *Biochem. J.* 1988, **256**, 1013–1019
- Version 97, Molecular Simulations, Inc., San Diego, Calif. USA, <http://www.msi.com>
- Brooks, B.R., Bruccoleri, R.E., Olafson, B.D., States, D.J., Swaminathan, S., and Karplus, M. CHARMM: a program for macromolecular energy, minimization, and dynamics calculations. *J. Comput. Chem.*, 1983, **4**, 187–217
- Version 4.1.1. 1993, Wavefunction, Inc., Irvine, Calif. USA, <http://www.wavefun.com>

- 24 Ammon, H.L., Sherrer, C., and Eicher, T. 1,2-Dimethyl-4,4-triafulvenedicarbonitrile (code=MTFULC). *Acta Cryst. Sect. B* 1978, **34**, 3782–3784
- 25 Temme, B., Erker, G., Frohlich, R., and Grehl, M. Boron-induced formation of a methylenecyclopropene unit in the bis(cycloentadienyl)zirconium coordination sphere (code=HELSEW). *J. Chem. Soc. Chem. Commun.*, 1994, 1713–1714
- 26 Frei, B., Schweizer, W.B., Wolf, H.R., and Jeger, O. (code=TMSOCO) *Rec. Trav. Chim. Pays-Bas*, 1979, **98**, 271
- 27 Allen, F.H., and Kennard, O. 3D search and research using the Cambridge Structure Database. *Chem. Des. Autom. News*, 1993, **8**, 131–137
- 28 Version 4.0. 1998, Univ. of Calif. at San Francisco, San Francisco, Calif. USA
- 29 Muszbek, L., Yee, V.C., and Hevessy, Z. Blood Coagulation Factor XIII: Structure and Function. *Thromb. Res.* 1999, **94**, 271–305
- 30 Pedersen, L.C., Yee, V.C., Bishop, P.D., Pedersen, L.C., Le Trong, I., Teller, D.C., and Stenkamp, R.E. Transglutaminase factor XIII uses proteinase-like catalytic triad to crosslink macromolecules. *Protein Sci.* 1994, **3**, 1131–1135

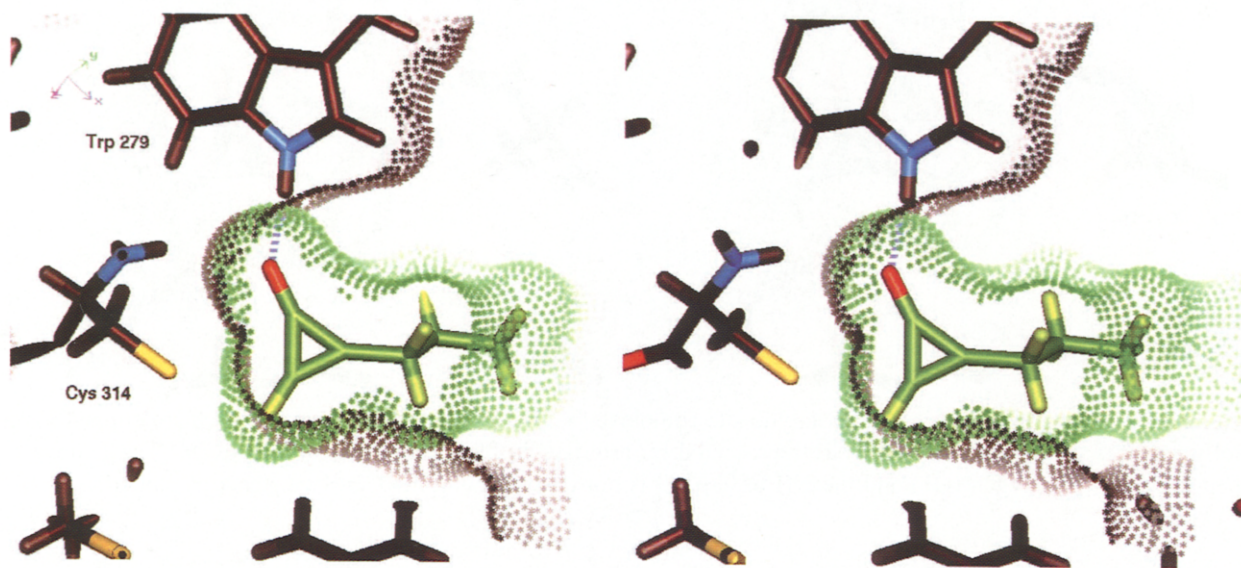
Conformational analysis and docking study of potent factor XIIIa inhibitors having a cyclopropenone ring



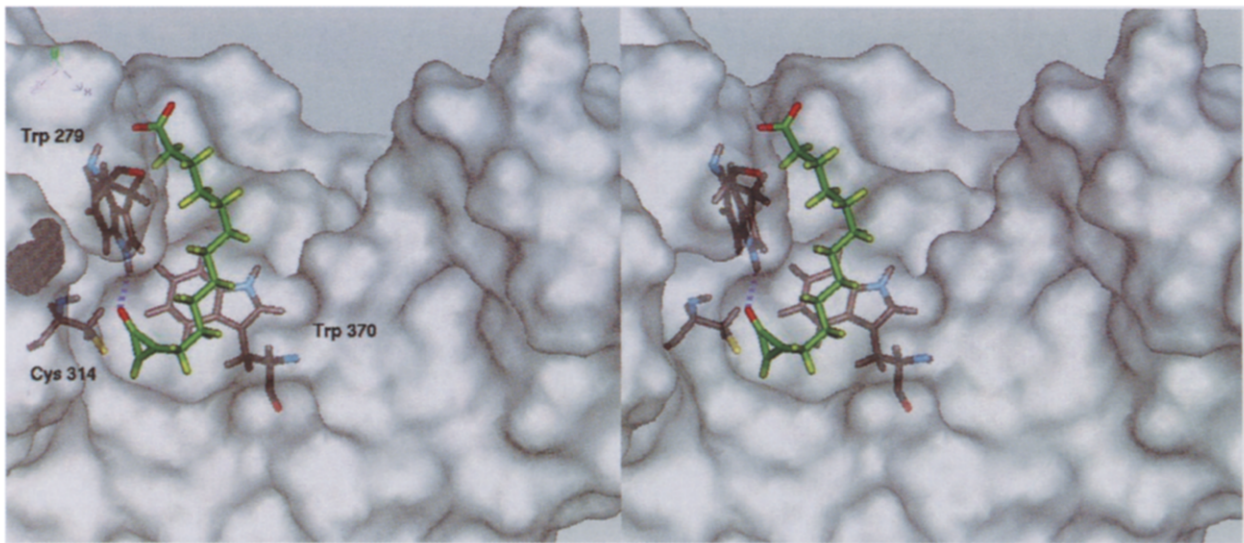
Color Plate 1. Stereo plot of the active site region of RmvB1. Residues within 10 Å from the sulfur atom of Cys314 are shown for clarity.



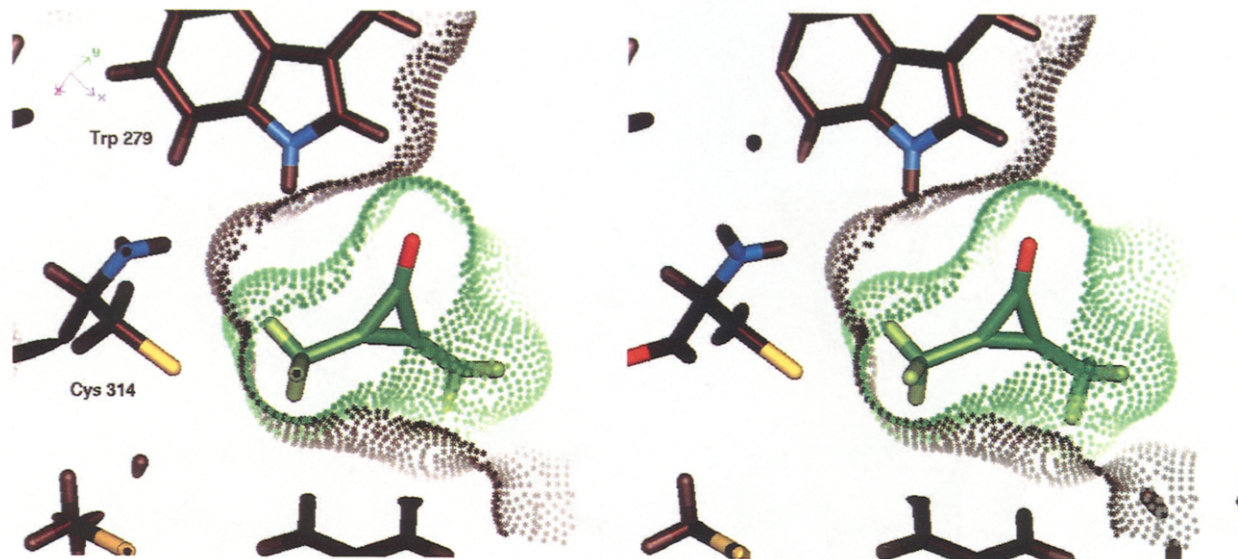
Color Plate 2. Complex structure model of the factor XIIIa binding site (black) and **5** (green) in site A. Connolly surface of the enzyme is shown in gray. A blue dotted line indicates the hydrogen bond between the carbonyl oxygen and the indole NH group of Trp279.



Color Plate 3. The magnified view of the catalytic site of Color Plate 2. The front and the back are clipped for clarity. Connolly surfaces of the enzyme and **5** are represented by asterisks in black and green, respectively. A blue dotted line indicates the hydrogen bond between the carbonyl oxygen (O1) and the indole NH group of Trp279. The terminal carbon atom (C2) of **5** is in close proximity to the sulfur atom ($S\gamma$) of Cys314 (The C2– $S\gamma$ distance is 2.9 Å).



Color Plate 4. Complex structure model of the factor XIIIa binding site (black) and **4** (green) in site B. Connolly surface of the enzyme is shown in gray. A blue dotted line indicates the hydrogen bond between O1 and the indole NH group of Trp279. The C2– $S\gamma$ distance is 3.1 Å.



Color Plate 5. The magnified view of the catalytic site complexed with **3** in site B. The front and back are clipped for clarity. Connolly surfaces of the enzyme and **3** are represented by asterisks in black and green, respectively. The hydrogen bond between the carbonyl oxygen (O1) and the NH of Trp279 is not observed and the C2-S γ distance is extended to 4.5 Å.